Published in final edited form as:
Nat Prod Rep. 2007 June ; 24(3): 610–620. doi:10.1039/b604194a.

Spectroscopic characterization of heme iron–nitrosyl species and their role in NO reductase mechanisms in diiron proteins†

Pierre Moënne-Loccoz
Department of Environmental & Biomolecular Systems, OGI School of Science and Engineering, Oregon Health & Science University, 20,000 NW Walker Road, Beaverton, Oregon, 97006-8921, USA. ploccoz@ebs.ogi.edu

Abstract

Nitric oxide (NO) plays an important role in cell signalling and in the mammalian immune response to infection. On its own, NO is a relatively inert radical, and when it is used as a signalling molecule, its concentration remains within the picomolar range. However, at infection sites, the NO concentration can reach the micromolar range, and reactions with other radical species and transition metals lead to a broad toxicity. Under aerobic conditions, microorganisms cope with this nitrosative stress by oxidizing NO to nitrate (NO_3^-). Microbial hemoglobins play an essential role in this NO-detoxifying process. Under anaerobic conditions, detoxification occurs *via* a 2-electron reduction of two NO molecules to N_2O. In many bacteria and archaea, this NO-reductase reaction is catalyzed by diiron proteins. Despite the importance of this reaction in providing microorganisms with a resistance to the mammalian immune response, its mechanism remains ill-defined. Because NO is an obligatory intermediate of the denitrification pathway, respiratory NO reductases also provide resistance to toxic concentrations of NO. This family of enzymes is the focus of this review. Respiratory NO reductases are integral membrane protein complexes that contain a norB subunit evolutionarily related to subunit I of cytochrome *c* oxidase (C*c*O). NorB anchors one high-spin heme b_3 and one non-heme iron known as Fe_B, *i.e*., analogous to Cu_B in C*c*O. A second group of diiron proteins with NO-reductase activity is comprised of the large family of soluble flavoprotein A found in strict and facultative anaerobic bacteria and archaea. These soluble detoxifying NO reductases contain a non-heme diiron cluster with a Fe–Fe distance of 3.4 Å and are only briefly mentioned here as a promising field of research. This article describes possible mechanisms of NO reduction to N_2O in denitrifying NO-reductase (NOR) proteins and critically reviews recent experimental results. Relevant theoretical model calculations and spectroscopic studies of the NO-reductase reaction in heme/copper terminal oxidases are also overviewed.

1 Nitric oxide reduction in biology

Hemoproteins play a dominant role throughout the chemistry of NO in biology. The production of NO from arginine by NO synthase depends on a heme cofactor, and regardless of whether NO is utilized as a secondary messenger, the regulatory domain of its target enzyme, guanylyl cyclase, also relies on a heme cofactor. Heme cofactors are equally crucial to the microbial response to toxic concentrations of NO by flavohemoglobins and other hemoglobin-like proteins under aerobic conditions. Here, we focus on a third branch of NO chemistry in biology: the reduction of NO to N_2O by hemoproteins (eqn 1).

†This paper was published as a part of a special issue on the chemistry and biochemistry of heme proteins.

$$2\,NO + 2\,H^+ + 2\,e^- \rightarrow N_2O + H_2O \quad (1)$$

The reactions by which NO is produced by reduction of nitrite (NO_2^-) and consumed by reduction to nitrous oxide (N_2O) are essential steps of the denitrification pathway. Respiratory NO reductases in true denitrifying organisms and in partial denitrifiers like the facultative anaerobes *Neisseria gonorrhoeae* and *Neisseria meningitidis*, provide these organisms with added resistance to toxic concentrations of NO.[1-3]

Denitrifying NO reductases (NOR) are integral membrane protein complexes for which there are no crystal structures yet available. The major subunit common to all denitrifying NORs, norB, is evolutionarily related to subunit I of cytochrome *c* oxidase (C*c*O). Specifically, the hydropathy pattern of C*c*O and the six histidine ligands of heme *a*, heme a_3, and Cu_B appear to be conserved in NORs.[4-6] Purification of NO reductases from a variety of denitrifying bacteria have confirmed that the NorB subunit (53 kDa) anchors one high-spin heme b_3 and one non-heme iron now known as Fe_B, in analogy with Cu_B in C*c*O.[5-9] Similar to the terminal oxidase superfamily, the NOR family exhibits variability in the electron-entry portion of the enzyme (Fig. 1).

The most extensively characterized subfamily of denitrifying NO reductases contains an additional NorC subunit (17 kDa), which binds a heme *c*; its members are referred to as cNORs.[8,10-12] NO reductases from *Ralstonia eutropha* and from the archaeon *Pyrobaculum aerophilum* are purified as single-component enzymes, which include quinol binding sites fused to their NorB subunits (84 kDa),[13,14] and are thus referred to as qNORs. Most strikingly, in *Bacillus azotoformans* (*B.a*. qCu_ANOR) two branches of electron acceptors coexist, a menaquinol binding site on NorB and a dinuclear copper site, Cu_A, on subunit II.[15-17]

In contrast to terminal oxidases, which couple the reduction of O_2 with translocation of protons across the membrane,[18] the catalytic cycle of cNOR is non-electrogenic.[19,20] Consequently, protons are supplied on the periplasmic side of the membrane, as are the electrons that originate from soluble and membrane-bound cytochrome *c*. Fully-reduced cNORs can complete two NO reductase catalytic cycles and have also been shown to reduce O_2 to H_2O.[21-23] UV-vis monitoring of the reaction of O_2 with fully-reduced cNOR reveals two major phases: one is assigned to O_2-binding to heme b_3 ($k = 2 \times 10^7\ M^{-1}\ s^{-1}$), and the second corresponds to the oxidation of the low-spin heme *b* and *c* ($k = 40\ s^{-1}$), a process which is coupled with proton uptake.[21,23]

By analogy with the mechanism of O_2 reduction in C*c*O and NOR, it is certainly reasonable to assume that NO binds at the dinuclear site composed by heme b_3 and Fe_B, and evidence to support this view continues to accumulate. Furthermore, it is possible to envisage several possible catalytic mechanisms. After a brief description of spectroscopic signatures of iron–nitrosyl species and of putative models for the NO reductase catalytic cycle, the most pertinent spectroscopic information obtained to date and its interpretation in terms of catalytic relevance will be reviewed.

2 Spectroscopic signatures of heme iron–nitrosyl complexes

In contrast to CO and O_2, NO coordinates both iron(II) and iron(III) species. In Enemark and Feltham formulism,[24] which counts metal d-electrons plus the lone π* electron from the nitrosyl ligand, iron(II)–NO and iron(III)–NO complexes are represented as $\{FeNO\}^7$ and $\{FeNO\}^6$ species, respectively. Crystal structures of metal–nitrosyl porphyrin complexes have shown that $\{MNO\}^6$ species adopt a linear M–N–O structure, while $\{MNO\}^7$ species

have bent M–N–O configurations.[24-26] Ferrous hemoproteins typically exhibit a very high affinity for NO while the ferric forms bind NO with K_d values in the micromolar range.[27-30] Because the concentration of NO during denitrification remains well below the micromolar range, it is assumed that the catalytic cycle of NO reductases is initiated by the binding of NO to an iron(II) in the reduced form of the enzyme.

Heme {FeNO}^{7} species are $S = 1/2$ species that can be reliably characterized by a combination of UV-vis, EPR and vibrational (resonance Raman (RR) and FTIR) spectroscopies. Specifically, 6-coordinate heme {FeNO}^{7} species display Soret absorbance at *ca*. 420 nm while 5-coordinate species exhibit blue-shifted Soret absorbance near 400 nm.[31-36] EPR signals for both coordination numbers are centered around $g = 2.0$, but show distinct superhyperfine splitting: a 3-line hyperfine structure is typically associated with a 5-coordinate heme–nitrosyl, whereas the added N-ligand of a proximal histidine in the 6-coordinated species induces further splitting to produce a 9-line hyperfine structure.[37,38] However, defining the coordination number of a {FeNO}^{7} species solely from EPR spectra may not be entirely foolproof. Indeed, in a recent study of NO binding to reduced heme/copper oxidase aa_3 from *Paracoccus denitrificans*, the characteristic 3-line hyperfine structure was not assigned to a 5-coordinate heme a_3 {FeNO}^{7} species, but rather to a 6-coordinate complex. In this case, the orientation of the Fe–N–O plane, with respect to the *trans*-imidazole plane, limits the involvement of the imidazole nitrogen p-orbital in the π-molecular orbital occupied by the unpaired electron, thus preventing further splitting of the 3-line hyperfine structure.[39]

In RR spectra, 6-coordinate {FeNO}^{7} species display ν_3 and ν_{10} porphyrin core modes at 1500 and 1630 cm^{-1}, respectively, while, in 5-coordinated species, these same modes are observed 5 to 10 cm^{-1} higher.[36,40-42] The ν(Fe–NO) and ν(NO) modes can be identified with isotopic labeling and provide further confirmation of the coordination number of the heme iron. Specifically, the proximal ligand *trans* to the nitrosyl has been shown to intensify the back-donation of Fe d_π electrons into the nitrosyl π* orbital, thus resulting in higher ν(Fe–NO) and lower ν(NO) for 6-coordinate species.[43] The distal pocket environment further modulates the extent of π-backbonding within the FeNO unit. While there are only a few fully characterized 6-coordinate {FeNO} models,[25,26] extensive studies of carbonyl synthetic models have led to a convincing description of distal perturbations on π-backbonding in heme Fe–CO complexes.[44-46] In hemoproteins, the control of the distal pocket environment on the extent of backbonding is equivalent in 6-coordinate {FeNO}^{7} species and Fe–CO complexes, as demonstrated by linear correlations between ν(NO)s and ν(CO)s, with slopes near unity for a series of distal pocket variants in myoglobin.[43,47,48] As is known for carbonyl complexes, polar environments and hydrogen-bond donation to the nitrosyl group have been shown to promote greater backbonding by stabilizing electron density on NO, thus leading to lower ν(NO) frequencies. The analysis of low-frequency Fe–N–O vibrational modes are more elusive since the intrinsically bent geometry of the {FeNO}^{7} unit provides greater flexibility to the nitrosyl group and results in extensive mixing of the ν(Fe–NO) and δ(Fe–N–O) modes.[49]

Heme {FeNO}^{6} species can be viewed as $S = 0$ low-spin iron(II)–NO^+ complexes that are isoelectronic with iron(II)–CO complexes. Accordingly, these species are EPR silent, and the Fe–N–O unit is usually linear with ν(NO) > 1900 cm^{-1}. Both 6- and 5-coordinate {FeNO}^{6} porphyrinate models have been characterized, but in proteins, only 6-coordinate species are known.[25,26] Electronic absorption spectra of {FeNO}^{6} in hemoproteins can be difficult to differentiate from those of their {FeNO}^{7} counterparts, and are sometimes strikingly similar.[50] Porphyrin skeletal vibrations observed in the high-frequency range of RR spectra, obtained with Soret excitations support a low-spin description of {FeNO}^{6} complexes.[30,50-54] The ν_3 and ν_{10} porphyrin core modes are observed at higher frequencies in {FeNO}^{6}

than in 6-coordinate {FeNO}^{7} species.[30,50-54] Importantly, vibrational modes of the FeNO unit in {FeNO}^{6} species do not seem to correlate with those of {FeNO}^{7} and carbonyl complexes. In fact, ferric–nitrosyl complexes in P450cam, with various substrates bound in the distal pocket, reveal a direct correlation between ν(Fe–NO) and ν(NO) rather than the inverse correlation observed between ν(Fe–XO) and ν(X–O) (*i.e.*, where X = N or C) in {FeNO}^{7} and carbonyl complexes.[49,53] Recently, Rodgers and coworkers extended these studies of P450-like enzymes to include other porphyrin {FeNO}^{6} systems using density function theory calculations.[55,56] Their results provide descriptions of higher-occupied molecular orbitals and their bonding characters, with respect to the Fe–NO and N–O bonds, in an effort to define relationships between observed vibrational frequencies, electronic structures, and reactivity.

3 Putative reaction mechanisms

The catalytic mechanism of NO reduction in dinuclear proteins can be divided into four steps: the initial coordination of NO at the diiron active site, the formation of an N–N bond, the cleavage of an N–O bond and the release of N_2O. In terms of the first two steps, three possible mechanisms have been proposed (Fig. 2).

3.1 *trans*-Mechanism

The catalytic cycle of this mechanistic model is initiated by the binding of two NO molecules at the diiron(II) cluster to form an iron–nitrosyl dimer [{FeNO}^{7}]$_2$ intermediate. The close proximity of the two metal–nitrosyl species promotes N–N bond formation either *via* an electrophilic attack by one nitrosyl at the nitrogen lone pair of the second nitrosyl, or *via* a radical coupling process, where the two nitrosyls combine to form a metal bound hyponitrite species ($N_2O_2^{2-}$). Several experimental observations support a *trans*-mechanism, including the characterization of an $(FeCO)_2$ heme/non-heme dicarbonyl complex at the active site of *B.a.* qCu_ANOR.[57] Also, rapid-freeze quench samples from single turnover reactions in cNOR have revealed EPR signals consistent with the trapping of S = 1/2 low-spin heme {FeNO}^{7} and S = 3/2 non-heme {FeNO}^{7} species.[58]

3.2 *cis*–Fe_B mechanism

This mechanism is characterized by the binding of two NO molecules at the non-heme iron center to form a dinitrosyl complex.[59] Dinitrosyl iron complexes exhibit isotropic g = 2.0 EPR signals and can be described as {Fe$(NO)_2$}^{9} species.[60,61] In this mechanistic model, the role of the heme iron would be limited to electron transfer, although interactions with the putative hyponitrite complex may participate in the N–O bond cleavage. The *cis* mechanism has been strongly favored by Thomson and coworkers because it does not involve the formation of a heme *b* {FeNO}^{7} species, which they view as a potential dead-end product.[62-65] Indeed, in many hemoproteins, ferrous–nitrosyl complexes are unreactive species.[66-70] Redox titrations of cNOR by Thomson and coworkers have indicated that the redox potential of heme b_3 is 200 mV more negative than that of the non-heme iron Fe_B, suggesting that a three-electron reduced state, where heme b_3 remains oxidized, may be relevant to catalysis.[64,65]

3.3 *cis*-Heme b_3 mechanism

In this mechanism, a heme b_3 {FeNO}^{7} species forms before reacting with a second NO molecule. The lone electron pair of the metal-bound nitrosyl is then the target of an electrophilic attack by a free NO to generate a hyponitrite radical. The reduction of the $N_2O_2^-$ group to hyponitrite may occur subsequently to the formation of an asymmetrically-bridged diiron cluster. This reaction mechanism is exemplified in the Pd/Cu-catalyzed reduction of NO in aqueous solution where, in a rate limiting step, cuprous salt reduces the

dinitrogen dioxide $PdCl_3(N_2O_2)^{2-}$ to give $PbCl_4^-$, N_2O, and water.[71] The *cis*-heme b_3 mechanism is also reminiscent of flavohemoglobin, if the initial $\{FeNO\}^7$ species in NOR is seen as analogous to the initial superoxo complex $\{FeO_2\}^8$ in flavohemoglobin. This mechanism has been suggested for the NO reductase activity in terminal oxidases where a heme $\{FeNO\}^7$ species accumulates in pseudo-steady state conditions.[72,73]

The timing of the N–O bond cleavage and protonation events that follow the N–N bond formation remain to be defined. Isomerization of putative transient hyponitrites to an O-coordinated species to promote the formation of a bridging oxo group and release of N_2O may be energetically unfavorable.[73] However, an O-coordination of the hyponitrite dianion to Fe_B could lead to N–O bond cleavage and formation of a $Fe_B(VI)=O$.[74] Alternatively, protonation of the hyponitrite anion (or a hyponitrite radical precursor) by a catalytic acid could favor the heterolytic cleavage of the N–O bond.

4 Spectroscopic characterization of denitrifying NO reductases

4.1 The diiron cluster can accommodate an Fe–Fe distance ≤ 3.5 Å

As is often the case with heme-containing proteins, RR spectroscopy was instrumental in providing unequivocal support for the similarities between NO reductases and C*c*O and for the presence of a heme/non-heme dinuclear cluster at the active site of NO reductase. Similar to the heme a_3 of C*c*O, RR spectra of fully reduced *P.d.* cNOR defined the heme b_3 as a 5-coordinate high-spin heme. Moreover, the detection of an iron(II)–N_{His} stretching mode at 218 cm^{-1} identified the heme b_3 axial ligand as a neutral histidine side chain.[11] In the oxidized enzyme, the presence of a μ-oxo-group bridging the two iron(III) centers was revealed by isotopic exchange with ^{18}O-labeled water.[75] Comparison of the iron(III)–O–iron(III) stretching frequency observed in *P.d.* cNOR with other *ν*(Fe–O–Fe) vibrations in non-heme diiron models[76] and a synthetic heme/non-heme synthetic model ($[(^5L)Fe^{III}–O–Fe^{III}–Cl]^+$)[77] provided the first direct evidence of a diiron cluster with an Fe–Fe distance ≤ 3.5 Å (Fig. 3).[75] Because the heme iron is 5-coordinate in both oxidized and reduced cNOR, and because a *ν*(Fe–N_{His}) was identified only in the reduced enzyme,[11] we concluded that the μ-oxo bridge must be hydrolyzed upon reduction, allowing for the coordination of the proximal histidine to heme b_3 and leaving an open coordination site facing Fe_B.[75]

The μ-oxo bridged diiron(III) cluster observed in *P.d.* cNOR is associated with a ligand-to-metal charge transfer absorption band at 595 nm. A lack of variation in both this absorption band and spectral features in the RR spectra suggest that the cluster is insensitive to pH changes between 6.0 and 9.0.[75,78] Mediated redox potentiometry has shown that the heme b_3 presents an unexpected low midpoint potential (E_m = 60 mV), which allows for the formation of a three-electron reduced form of the enzyme where the heme b_3 remains as the sole iron(III) species.[64] Room temperature absorption and MCD analyses of the three-electron reduced enzyme at different pH values suggest that, upon reduction of Fe_B, the μ-oxo bridge dissociates from Fe_B(II) and the heme b_3 iron(III) rebinds the proximal histidine to form a 6-coordinate aquo/hydroxo complex with charge transfer bands at 635 and 605 nm, respectively.[78] Not surprisingly, cyanide was shown to bind much more readily to heme b_3 in the three-electron reduced form of the enzyme, where the displacement of the sixth aquo/hydroxo ligand is facile (*e.g.*, as in metmyoglobin), than in the fully oxidized enzyme, where the μ-oxo group bridge between the two iron(III) is quite stable.[65] From these observations, Thomson and coworkers proposed that the μ-oxo bridged diiron(III) cluster might represent a “closed” resting state of the enzyme, while the catalytic cycle may, in fact, be initiated by the binding of NO to the mixed valence heme b_3(III)–Fe_B(II) cluster.[64,65,78]

Regardless of whether the diiron(III) μ-oxo bridge cluster is part of the catalytic cycle of NO reductases, this structure reveals a metal–metal distance that is 1.5 Å shorter that that

measured in the crystal structures of terminal oxidases between the iron of heme a_3 and Cu_B.[79-83] This significant distinction between the active sites of *P.d.* cNOR and C*c*O may explain their different reactivity toward NO. The iron–iron distance in NOR is more comparable with those measured for the carboxylate-bridged non-heme diiron clusters of the R2 subunit of *E. coli* ribonucleotide reductase, methane monooxygenase,[84-86] and flavoprotein A.[87] Interestingly, NO-reductase activity has been reported in all three of these diiron proteins.[88-90] The characterization of fully-oxidized and fully-reduced *P.d.* cNOR makes clear that the proximal histidine is labile and suggests that the catalytic intermediate might include a pentacoordinated heme $\{FeNO\}^7$ species. Structural characterizations of iron(II)–nitrosyl porphyrin complexes by Scheidt and coworkers have shown that, as the proximal ligand is released, the iron is pulled further out of the porphyrin plane by 0.2 Å, while the Fe–N and N–O distances and the Fe–N–O angle decrease only slightly.[25,26,91] The latter changes are consistent with a modest strengthening of both σ and π bonding in the FeNO unit. A recent crystal structure of nitrosyl–hemoglobin in the presence of the effector inositol hexaphosphate concurs with the iron displacement measured in model complexes.[92] Specifically, in β-subunits where 6-coordinated $\{FeNO\}^7$ species form, the iron remains 0.12 Å out of the porphyrin plane on the proximal side, however, in α-subunits where 5-coordinated $\{FeNO\}^7$ species form, the iron is located 0.25 Å out of the porphyrin plane toward the distal side. At the dinuclear site of NO reductases, a 5-coordinate $\{FeNO\}^7$ structure at the heme b_3 would decrease the distance between the nitrosyl group and a second $\{FeNO\}^7$ species at Fe_B, a change that may favor radical coupling and N–N bond formation.

4.2 The diiron site can accommodate two CO molecules

Carbon monoxide (CO) is an ideal probe to investigate the binding of exogenous diatomic ligands at the dinuclear site of NO reductases. Heme iron–carbonyl complexes are stable and exhibit a characteristic ν(C–O) between 1940 and 1980 cm^{-1} in RR and FTIR spectra.[93] Moreover, heme iron–carbonyls are photolabile and can be used to probe the heme distal pocket. In myoglobin, for example, the photolyzed CO can be trapped in several docking sites within the distal pocket.[94-96] These photolyzed CO molecules in proteinaceous docking sites display weak, but well-resolved, ν(C–O) near 2130 cm^{-1} in low-temperature FTIR spectra.[97-99] In terminal oxidases, CO dissociates from heme a_3 and coordinates to Cu_B. The Cu_B–CO complex can be trapped at cryogenic temperatures, and 'dark' minus 'illuminated' FTIR difference spectra exhibit a positive ν(CO) from the a_3–CO complex and a negative ν(CO) between 2040–2070 cm^{-1} characteristic of Cu_B–CO.[100-103]

In 1998, Saraste and coworkers attempted to use this approach with *P.d.* cNOR and reported that FTIR difference spectra could only be observed between dark and continuous illumination at 234 K.[104] The asymmetric absorption changes, centered around 1970 cm^{-1}, were interpreted in terms of a 'dark' signal at 1977 cm^{-1}, assigned to heme b_3–CO, and a 'light' signal at 1963 cm^{-1}, assigned to Fe_B–CO. However, these absorption changes may, in fact, originate from variations in populations of heme a_3–CO conformers under continuous illumination rather than CO-coordination to Fe_B. FTIR difference spectra between *P.d.* cNOR–^{12}CO and cNOR–^{13}CO obtained at Oregon Health & Science University confirmed that only one CO molecule binds per diiron site.[105] 'Dark' minus 'illuminated' FTIR difference spectra at 15 K exhibit a 'dark' ν(CO) at 1972 cm^{-1}, assigned to heme b_3–CO, and an 'illuminated' ν(CO) signal at 2120 cm^{-1} that is characteristic of non-coordinated CO docking at the hydrophobic site near the distal pocket.[105] Thus, from these FTIR experiments, it remains unclear whether CO can bind Fe_B following photolysis from heme b_3 in *P.d.* cNOR.

The CO photolysis in *P.d.* cNOR was also investigated at room temperature using time-resolved electronic absorption. These experiments revealed a very fast recombination rate

(k_{on} = 1.7 × 10^8 M^{-1} s^{-1}), approximately three orders of magnitude faster than in terminal oxidases.[106] In contrast, when Watmough and collaborators measured the rate constant for the initial binding of CO by stopped-flow spectroscopy, they observed a much slower rate (k_{on} = 1.2 × 10^5 M^{-1} s^{-1}).[106] The authors suggested that binding of CO at the heme a_3 requires the initial displacement of a distal heme ligand. The slow rebinding of this ligand, compared to CO, would explain the photolysis kinetics.[106] However, RR studies identify the ferrous heme b_3 as a 5-coordinate high-spin species,[11,107] thus, the kinetic data may be consistent with the presence of a weakly interacting group that can adopt variable configurations rather than with the displacement of a true distal ligand of heme b_3 (*vide infra*).

In sharp contrast with *P.d.* cNOR–CO, recent experiments with the CO complex of qCu_ANOR show that two CO molecules bind concomitantly at the diiron site of qCu_ANOR.[57] Specifically, room temperature (^{12}CO minus ^{13}CO) FTIR difference spectra of qCu_ANOR–CO show two ν(CO) modes at 1972 and 2068 cm^{-1} (Fig. 4). The band at 1972 cm^{-1} ($\Delta^{13}CO$=−44 cm^{-1}) corresponds to a heme–CO and is nearly identical to that observed in the heme–CO complex of *P.d.* cNOR.[11,105,108] The ν(CO) at 2068 cm^{-1} ($\Delta^{13}CO$ = −47 cm^{-1}) is consistent with a non-heme iron–CO where the back-bonding donation from the iron d_π orbitals to the carbonyl π^* orbitals is weakened compared to its heme–CO counterparts. The comparable integrated area of these two bands suggests that these two species are present in equivalent concentrations. These room temperature data may be interpreted in two ways: i) two CO molecules occupy the dinuclear active site, or ii) the active site contains only one CO molecule in a binding equilibrium between the heme and the non-heme irons. However, the comparison of the integrated areas of the room temperature signals with the total enzyme concentration favors the first alternative, and low-temperature photolysis experiments confirm this conclusion.[57]

The ‘dark’ minus ‘illuminated’ FTIR difference spectrum of qCu_ANOR–CO obtained at 15 K (Fig. 4) shows a positive cluster of bands centered around 1972 cm^{-1} that is assigned to comparable conformers of the photolabile heme–CO complex. A new band at 1910 cm^{-1} ($\Delta^{13}CO$ = −44 cm^{-1}), which is not observed at room temperature, is characteristic of a semi-bridging configuration between two metal ions.[93] Accompanying this band is an *S*-signal with a positive band at 2046 cm^{-1} and a negative band at 2066 cm^{-1} (Fig. 4). The influence of temperature on the FTIR difference spectra shows the interdependence of these two signals. Indeed, as the temperature is raised to ~100 K, the 1972 cm^{-1} signal decreases as geminate rebinding begins to occur, but the 1910 cm^{-1} band and the 2046/2066 cm^{-1} *S*-signal are unchanged. We have assigned the *S*-signal to a downshift of the non-heme Fe_B–CO as it is perturbed by the photolysis of the semi-bridging heme–CO at 1910 cm^{-1} (Fig. 4).[57] These results lend support to the *trans*-mechanistic model in which N–N bond formation is promoted by the binding of two NO molecules to form a $[\{FeNO\}^7]_2$ transient species.

Upon addition of chloride to qCu_ANOR–CO, the binding of CO at the Fe_B site is inhibited (Fig. 4), and the FTIR characterization of qCu_ANOR–CO resembles that of *P.d.* cNOR–CO. Similarly, in the heme/non-heme synthetic model $[(^6L)–Fe^{II} \ldots Fe^{II}–(Cl)]^+$, CO binding occurs at the heme iron, but the non-heme iron(II) does not bind CO, at least in part because of the chloride coordination.[109] It remains unclear in the case of NOR, whether, chloride directly binds to Fe_B(II) or whether its affect on Fe_B(II) ligation is only allosteric, but control experiments suggest that different states of the diiron site cannot solely be explained by the effect of chloride.[105,110] Thus, in both NOR proteins, there is clear experimental evidence for the presence of a yet unidentified ligand(s) that can adopt variable coordination geometries. At this time, it is tempting to speculate that a glutamate side chain at the diiron site might provide coordination flexibility to this site. Several glutamate residues are conserved in norB while absent from subunit I in terminal oxidases.[4-6] In particular,

conserved residues Glu198 and Glu202 (numbering from *P. denitrificans* norB) are located in transmembrane helix VI, which includes His194, a putative ligand to Fe_B. Moreover, the RR characterizations of the CO complexes of *P.d*. cNOR and qCuANOR suggest the presence of negatively charged residues in the distal pocket of heme b_3.[11,105]

Richardson and coworkers have engineered expression systems from norB variants in *P. denitrificans* and *E. coli* and analyzed the NO reductase activity of membrane fragments and solubilized proteins.[22] Three mutants of conserved glutamate residues were successfully expressed and purified: E198A and E202A, which are expected to be at or near the diiron active site, and E125A, which is predicted to be on the periplasmic surface. The location of Glu125, and the loss of NO reductase activity in E125A suggest that this residue may play a role in proton transfer from the periplasm to the active site. While E202A shows an NO-reductase activity comparable to the wild type protein, the E198A variant is inactive. These results suggest that E198 plays an important role at the diiron active site, either as a ligand to Fe_B or as a proton transfer group.

In non-heme diiron proteins, X-ray crystallography has revealed variations in the coordination of carboxylate groups that accompany changes in the oxidation state of the diiron cluster. For example, in the R2 subunit of *E. coli* ribonucleotide reductase and in methane monooxygenase, a coordinating glutamate side chain switches from bridging the two irons in the fully-reduced enzymes to terminally coordinating a single iron(III) in the oxidized proteins.[111-116] Variations in carboxylate coordination geometry also take place without changes in iron oxidation states. For example, interactions of regulatory subunits such as MMOB with the hydroxylase protein of methane monooxygenase and acyl carrier protein with Δ^9-desaturase affect the spectroscopic characteristics of the diiron(II) cluster at the active site.[117-119] These observations led to the concept of carboxylate shifts controlling the number of open coordination sites and the range of Fe–Fe distances during catalytic turnover.[120] Thus, in NOR, where glutamate side chains in the vicinity of coordinating histidine residues are known to be conserved, it is conceivable that carboxylate shifts might control the coordination of diatomic molecules at the heme/non-heme diiron site.

4.3 Spectroscopic studies of NO reactions with NOR

Using rapid-freeze quenching, Shiro and coworkers have shown that NO and fully-reduced cNOR react in a sub-millisecond time scale, as evidenced by the appearance of new EPR signals within 0.5 ms after mixing.[58] One signal, at $g = 4$, is consistent with a non-heme $S = 3/2$ $\{FeNO\}^7$ species, and another at $g = 2.01$, with a pronounced 3-line hyperfine structure, is characteristic of a heme $S = 1/2$ $\{FeNO\}^7$ system. Shiro and coworkers estimate that these two nitrosyl signals represent 30% of the total diiron site concentration. In addition, they show that these species decay within 10 ms when their EPR signatures are replaced with those of ferric low-spin *b* and *c* hemes.[58] The data have been interpreted in terms of a *trans*-mechanism where a $[\{FeNO\}^7]_2$ unit forms at the active site within the first ms after mixing.[58]

The observation of a $g = 4$ signal from a non-heme $\{FeNO\}^7$ species and a $g = 2.0$ signal from a heme $\{FeNO\}^7$ upon addition of NO to fully-reduced cNOR had been reported earlier in hand-mixing experiments,[104] but their relevance to the native structure have been seriously questioned as these EPR signals appeared to increase under prolonged incubation.[121] In contrast with hand-mixed experiments, the millisecond kinetics of the formation and decay of the EPR signals observed by Shiro and coworkers support the involvement of these species in the catalytic cycle of NOR.[58] The interpretation of these EPR data may be revisited however, as one might expect a heme/non-heme $[\{FeNO\}^7]_2$ complex to be magnetically coupled to form an EPR-silent spin integer species (most likely antiferromagnetically coupled, *i.e.*, an $S = 1$ system). For example, the major species formed

by the reaction of NO with the reduced non-heme diiron site of protein R2 is an EPR-silent, antiferromagnetically-coupled $[\{FeNO\}^7]_2$ complex.[88,122] Shiro and coworkers favor the formation of an $[\{FeNO\}^7]_2$ unit on the basis that the $g = 4$ signal of the reaction intermediate behaves differently, with respect to microwave power saturation, than in the CO-inhibited species, where the $S = 0$ low-spin iron(II) carbonyl complex does not promote relaxation.[58] However, an increase in relaxation would be expected whether or not NO binds to heme b_3 since both heme $\{FeNO\}^7$ and high-spin iron(II) are $S \neq 0$ species. An alternative to the authors' proposal may be that within the first millisecond after exposure of fully-reduced cNOR to NO a mixture of [heme b_3 Fe–NO/Fe_B] and [heme b_3 Fe/Fe_B–NO] complexes can be produced. Indeed, if the metal centers are magnetically uncoupled upon complexation with a single NO molecule, both $S = 3/2$ and $S = 1/2$ $\{FeNO\}^7$ species are expected to contribute to the EPR spectra. This alternative interpretation would imply that the two iron(II) ions at the active site pocket have comparable binding affinity for NO, and that these $\{FeNO\}^7$ complexes can be trapped by rapid-freeze quenched techniques. A $[\{FeNO\}^7]_2$ complex, on the other hand, might not be observable by EPR, or it might not accumulate in the course of a single turnover reaction. The concept of a mixture of {FeNO} complexes has support from the evolutionarily-related cytochrome ba_3 oxidase from *T. thermophilus*, from which FTIR experiments have revealed an [heme b_3 Fe–CO/Cu_B] ↔ [heme b_3 Fe/Cu_B–CO] equilibrium.[123] In addition, theoretical analyses of the *in silico* reduction of NO with simplified heme/copper and heme/non-heme dinuclear clusters calculate reaction-energy profiles where hyponitrite, rather than dinitrosyl complexes, are the observable intermediates.[73,74] Thus, two CO molecules bound at the diiron site of NOR can be observed as the complex is stable in qCu_ANOR,[57] but a $[\{FeNO\}^7]_2$ transient might not be a traceable intermediate if it does not accumulate in the course of the reaction.

NO can also react with fully-oxidized *P.d.* NOR,[10,124] but this reaction only occurs at pH < 6, where acidic conditions presumably favor the hydrolysis and displacement of the μ-oxo bridge to allow NO coordination to heme b_3.[125] The heme b_3 $\{FeNO\}^6$ species displays a ν(Fe–NO) at 594 cm^{-1} and a ν(NO) at 1904 cm^{-1}.[124] These stretching frequencies are at the low range of those reported for 6-coordinate heme $\{FeNO\}^6$ species with a proximal histidine ligand.[30,50,51,54,126-128] Varotsis and coworkers[124] noted that the low ν(NO) contrasts with the high ν(CO) associated with inhibition of π-backbonding in the negative polarity of the distal pocket.[11] As discussed earlier (see section 2; spectroscopic signatures of heme iron–nitrosyl complexes), the influence of distal pocket environment on the characteristics of heme $\{FeNO\}^6$ species remains poorly understood.[55,56] It is also unclear whether or not the heme b_3 $\{FeNO\}^6$/Fe_B(III) state is relevant to the catalytic cycle of NOR.

5 NO reduction in terminal oxidases

The various reactions of NO with heme/copper terminal oxidases and their importance to the regulation process of O_2-respiration have been recently reviewed.[129-132] Briefly, the interaction of NO with the oxidized enzyme inhibits mitochondrial C*c*O *via* binding of NO to Cu_B(II).[133,134] The resulting copper–nitrosyl complex adopts a Cu_B(I)–NO^+ configuration and produces nitrite upon hydration of the bound nitrosonium ion.[129,135-137] In contrast, reduced terminal oxidases bind NO in a competitive fashion with O_2 to form a heme a_3 $\{FeNO\}^7$ complex.[138] In some terminal oxidases, experimental observations corroborate the concomitant binding of a second NO molecule at the Cu_B(I) site. For example, FTIR experiments by Caughey and coworkers on reduced bovine C*c*O exposed to NO revealed two ν(NO)s at 1610 and 1700 cm^{-1}, which were assigned to heme a_3-NO and Cu_B-NO, respectively.[139] In addition, optical experiments monitoring rebinding dynamics in the picosecond time scale for the NO complex of reduced aa_3 from *P. denitrificans* showed that geminate rebinding to the heme a_3 site is predominant at high NO concentration. This behavior was assigned to an obstruction of the exit route for the photolyzed NO by a second

NO bound to Cu_B.[39] It is interesting to note that while these metal–nitrosyl Fe/Cu dimers in C*c*O and aa_3 mimic the putative $[\{FeNO\}^7]_2$ intermediate in NOR, neither of these terminal oxidases show any NO reductase activity.

The fully-reduced caa_3 and ba_3 oxidases from *Thermus thermophilus* quickly react with NO to form a heme a_3 $\{FeNO\}^7$ complex, which decays to produce N_2O with a turnover rate approximately 1% and 0.1% that of denitrifying NORs, respectively.[138,140] Presumably, binding of a second NO to $Cu_B(I)$ is slow and results in a facile turnover to form N_2O.[39,72] Thus, binding of a second NO molecule may occur in all oxidases, but the only catalytically competent dinitrosyl complexes form in *T. thermophilus* oxidases. All fully-reduced terminal oxidases react with NO to form a heme $\{FeNO\}^7$ complex that can be spectroscopically characterized.[130,131,141] While both 5-coordinate and 6-coordinate $\{FeNO\}^7$ hemes have been reported in terminal oxidases,[39,72,142] the coordination number of the heme iron does not appear to correlate with NO reductase activity.[138,140]

The heme iron–nitrosyl complex in *T. thermophilus* ba_3 has been studied by time-resolved absorption spectroscopy and displays rebinding dynamics on the 15 ns time scale at room temperature.[39] This relatively slow rebinding process suggests that the photolyzed-NO group binds transiently to another site, presumably Cu_B. Time-resolved step-scan FTIR spectra of the heme a_3–NO complex in *T. thermophilus* ba_3 after flash photolysis show no differential signals and indicate that rebinding occurs within the 5-μs time resolution of this technique.[143] Using density function theory calculations, and within the context of a *trans*-mechanism, Varotsis and coworkers have proposed that the formation of a [heme a_3-NO – Cu_B-NO] dinitrosyl complex leads to an *N*,*N*′-bridging hyponitrite intermediate.[144] Using the same theoretical approach, Blomberg and coworkers favor a *cis*-heme a_3 mechanism and a bridging coordination of the hyponitrite to form a 5-member ring with two O-atoms coordinated to Cu_B.[73] Although only a few transition metal hyponitrite complexes have been structurally characterized to date,[145-148] these complexes already demonstrate a wide diversity in coordination geometries. There is little doubt that the characterization of a hyponitrite intermediate in the reaction of fully-reduced ba_3 with NO would constitute a major breakthrough toward understanding these catalytic reactions.

6 Conclusions and perspectives

Structural and functional similarities between NO reductases and the heme/copper terminal oxidases are now firmly established, and in view of the existing literature on terminal oxidases, the existence of different forms of NORs is not surprising. Indeed, resting and pulsed/fast forms of oxidized and reduced C*c*O are well documented.[149] The effect of chloride on the family of terminal oxidases is notoriously complex and ranges from direct binding to cuprous $Cu_B(I)$,[150-152] to bridging the heme a_3 iron(III) and $Cu_B(II)$,[149,153] to binding at heterotropic sites.[149,154,155] With its poor NO reductase activity and access to its three-dimensional structure, *T. thermophilus* cytochrome ba_3 provides an opportunity to gather spectroscopic information on NO reaction intermediates. Nevertheless, because of their different metal composition, what is learned from heme/copper terminal oxidase systems will not always be applicable to NORs. A clear definition of the catalytic cycle of NOR will require the combination of rapid-freeze quenching and multiple spectroscopic techniques.

Several carboxylate-bridged non-heme diiron proteins catalyze the reduction of NO to N_2O, and the flavoprotein A family of enzymes has recently been exposed as detoxifying NO reductases.[90,156,157] A recombinant form of flavoprotein A from *Moorella thermoacetica*, which exhibits comparable NO reductase activity to denitrifying NORs, was recently crystallized.[87] In this protein, the active site contains a non-heme diiron cluster with two

histidines per iron and two bridging ligands: a bidentate carboxylate group and a solvent molecule.[87] Carboxylate groups have been shown to provide structural flexibility at the active sites of non-heme diiron proteins (for an extreme example, see recent crystal structures of nigerythrin, which reveal a 2 Å movement of one iron associated with a Glu ↔ His ligand "toggling" at one iron[158]). In denitrifying NOR, Fe_B may likewise recruit a glutamate side chain as a ligand, which, in turn, may allow the site to control the reactivity of $\{FeNO\}^7$ species, regulate the catalytic cycle and prevent the formation of dead-end complexes through carboxylate shifts.

Acknowledgments

This work was supported by the National Institutes of Health (GM 074785). The contributions of students and colleagues at OHSU, Shen Lu, Hong-wei Huang, and I.-Jin Lin, are gratefully acknowledged. The author also expresses sincere thanks to his collaborators Simon de Vries, Kenneth D. Karlin, James A. Fee, and to members of their groups.

References

1. Lissenden S, Mohan S, Overton T, Regan T, Crooke H, Cardinale JA, Householder TC, Adams P, O'Conner CD, Clark VL, Smith H, Cole JA. Mol Microbiol 2000;37:839–855. [PubMed: 10972806]
2. Householder TC, Fozo EM, Cardinale JA, Clark VL. Infect Immun 2000;68:5241–5246. [PubMed: 10948150]
3. Anjum MF, Stevanin TM, Read RC, Moir JW. J Bacteriol 2002;184:2987–2993. [PubMed: 12003939]
4. Castresana J, Lübben M, Saraste M, Higgins DG. EMBO J 1994;13:2516–2525. [PubMed: 8013452]
5. van der Oost J, de Boer AP, de Gier JW, Zumft WG, Stouthamer AH, van Spanning RJ. FEMS Microbiol Lett 1994;121:1–9. [PubMed: 8082820]
6. Zumft WG, Braun C, Cuypers H. Eur J Biochem 1994;219:481–490. [PubMed: 7508388]
7. Heiss B, Frunzke K, Zumf WG. J Bacteriol 1989;171:3288–3297. [PubMed: 2542222]
8. Wasser IM, de Vries S, Moënne-Loccoz P, Schröder I, Karlin KD. Chem Rev 2002;102:1201–1234. [PubMed: 11942794]
9. Averill BA. Chem Rev 1996;96:2951–2965. [PubMed: 11848847]
10. Girsch P, de Vries S. Biochim Biophys Acta 1997;1318:202–216. [PubMed: 9030265]
11. Moënne-Loccoz P, de Vries S. J Am Chem Soc 1998;120:5147–5152.
12. Zumft WG. J Inorg Biochem 2005;99:194–215. [PubMed: 15598502]
13. Cramm R, Pohlmann A, Friedrich B. FEBS Lett 1999;460:6–10. [PubMed: 10571051]
14. de Vries S, Strampraad MJ, Lu S, Moënne-Loccoz P, Schröder I. J Biol Chem 2003;278:35861–35868. [PubMed: 12799376]
15. Suharti, Strampraad MJ, Schröder I, de Vries S. Biochemistry 2001;40:2632–2639. [PubMed: 11327887]
16. Suharti, Heering HA, de Vries S. Biochemistry 2004;43:13487–13495. [PubMed: 15491156]
17. Suharti, de Vries S. Biochem Soc Trans 2005;33:130–133. [PubMed: 15667284]
18. Ferguson-Miller S, Babcock GT. Chem Rev 1996;96:2889–2907. [PubMed: 11848844]
19. Shapleigh JP, Payne WJ. J Bacteriol 1985;163:837–840. [PubMed: 3928599]
20. Hendriks JH, Jasaitis A, Saraste M, Verkhovsky MI. Biochemistry 2002;41:2331–2340. [PubMed: 11841226]
21. Fujiwara T, Fukumori Y. J Bacteriol 1996;178:1866–1871. [PubMed: 8606159]
22. Butland G, Spiro S, Watmough NJ, Richardson DJ. J Bacteriol 2001;183:189–199. [PubMed: 11114916]
23. Flock U, Watmough NJ, Ädelroth P. Biochemistry 2005;44:10711–10719. [PubMed: 16060680]
24. Enemark JH, Feltham RD. Coord Chem Rev 1974;13:339–406.

25. Scheidt WR, Ellison MK. Acc Chem Res 1999;32:350–359.
26. Wyllie GR, Scheidt WR. Chem Rev 2002;102:1067–1090. [PubMed: 11942787]
27. Hoshino M, Ozawa K, Seki H, Ford PC. J Am Chem Soc 1993;115:9568–9575.
28. Abu-Soud HM, Ichimori K, Presta A, Stuehr DJ. J Biol Chem 2000;275:17349–17357. [PubMed: 10749853]
29. Laverman LE, Wanat A, Oszajca J, Stochel G, Ford PC, van Eldik R. J Am Chem Soc 2001;123:285–293. [PubMed: 11456515]
30. Wang J, Lu S, Moënne-Loccoz P, Ortiz de Montellano PR. J Biol Chem 2003;278:2341–2347. [PubMed: 12433915]
31. Yoshimura T, Ozaki T. Arch Biochem Biophys 1984;229:126–135. [PubMed: 6703691]
32. Yoshimura T, Suzuki S, Nakahara A, Iwasaki H, Masuko M, Matsubara T. Biochemistry 1986;25:2436–2442.
33. Coletta M, Boffi A, Ascenzi P, Brunori M, Chiancone E. J Biol Chem 1990;265:4828–4830. [PubMed: 2318864]
34. Stone JR, Marletta MA. Biochemistry 1994;33:5636–5640. [PubMed: 7910035]
35. Decatur SM, Franzen S, DePillis GD, Dyer RB, Woodruff WH, Boxer SG. Biochemistry 1996;35:4939–4944. [PubMed: 8664286]
36. Reynolds MF, Parks RB, Burstyn JN, Shelver D, Thorsteinsson MV, Kerby RL, Roberts GP, Vogel KM, Spiro TG. Biochemistry 2000;39:388–396. [PubMed: 10631000]
37. Palmer, G. The porphyrins. Dolphin, D., editor. Vol. IV. Academic Press; New York: 1979.
38. Hille R, Olson JS, Palmer G. J Biol Chem 1979;254:12110–12120. [PubMed: 40990]
39. Pilet E, Nitschke W, Rappaport F, Soulimane T, Lambry JC, Liebl U, Vos MH. Biochemistry 2004;43:14118–14127. [PubMed: 15518562]
40. Tsubaki M, Yu NT. Biochemistry 1982;21:1140–1144. [PubMed: 7074070]
41. Deinum G, Stone JR, Babcock GT, Marletta MA. Biochemistry 1996;35:1540–1547. [PubMed: 8634285]
42. Andrew CR, George SJ, Lawson DM, Eady RR. Biochemistry 2002;41:2353–2360. [PubMed: 11841228]
43. Vogel KM, Kozlowski PM, Zgierski MZ, Spiro TG. J Am Chem Soc 1999;121:9915–9921.
44. Kerr EA, Mackin HC, Yu NT. Biochemistry 1983;22:4373–4379. [PubMed: 6626507]
45. Li XY, Spiro TG. J Am Chem Soc 1988;110:6024–6033.
46. Ray GB, Li X-Y, Ibers JA, Sessler JL, Spiro TG. J Am Chem Soc 1994;116:162–176.
47. Park ES, Thomas MR, Boxer SG. J Am Chem Soc 2000;122:12297–12303.
48. Coyle CM, Vogel KM, Rush TS 3rd, Kozlowski PM, Williams R, Spiro TG, Dou Y, Ikeda-Saito M, Olson JS, Zgierski MZ. Biochemistry 2003;42:4896–4903. [PubMed: 12718530]
49. Hu S, Kincaid JR. J Am Chem Soc 1991;113:9760–9766.
50. Ding XD, Weichsel A, Andersen JF, Shokhireva TK, Balfour C, Pierik AJ, Averill BA, Montfort WR, Walker FA. J Am Chem Soc 1999;121:128–138.
51. Benko B, Yu NT. Proc Natl Acad Sci U S A 1983;80:7042–7046. [PubMed: 6580627]
52. Hu S, Kincaid JR. J Biol Chem 1993;268:6189–6193. [PubMed: 8384203]
53. Obayashi E, Tsukamoto K, Adachi S, Takahashi S, Nomura M, Iizuka T, Shoun H, Shiro Y. J Am Chem Soc 1997;119:7807–7816.
54. Tomita T, Haruta N, Aki M, Kitagawa T, Ikeda-Saito M. J Am Chem Soc 2001;123:2666–2667. [PubMed: 11456938]
55. Linder DP, Rodgers KR, Banister J, Wyllie GR, Ellison MK, Scheidt WR. J Am Chem Soc 2004;126:14136–14148. [PubMed: 15506779]
56. Linder DP, Rodgers KR. Inorg Chem 2005;44:1367–1380. [PubMed: 15732977]
57. Lu Suharti S, de Vries S, Moënne-Loccoz P. J Am Chem Soc 2004;126:15332–15333. [PubMed: 15563131]
58. Kumita H, Matsuura K, Hino T, Takahashi S, Hori H, Fukumori Y, Morishima I, Shiro Y. J Biol Chem 2004;279:55247–55254. [PubMed: 15504726]

59. Ye RW, Averill BA, Tiedje JM. Appl Environ Microbiol 1994;60:1053–1058. [PubMed: 8017903]
60. Bryar TR, Eaton DR. Can J Chem 1992;70:1917–1926.
61. Wang X, Sundberg EB, Li L, Kantardjieff KA, Herron SR, Lim M, Ford PC. Chem Commun 2005:477–479.
62. Butler CS, Seward HE, Greenwood C, Thomson AJ. Biochemistry 1997;36:16259–16266. [PubMed: 9405060]
63. Watmough NJ, Cheesman MR, Butler CS, Little RH, Greenwood C, Thomson AJ. J Bioenerg Biomembr 1998;30:55–62. [PubMed: 9623806]
64. Grönberg KL, Roldán MD, Prior L, Butland G, Cheesman MR, Richardson DJ, Spiro S, Thomson AJ, Watmough NJ. Biochemistry 1999;38:13780–13786. [PubMed: 10529222]
65. Grönberg KL, Watmough NJ, Thomson AJ, Richardson DJ, Field SJ. J Biol Chem 2004;279:17120–17125. [PubMed: 14766741]
66. Moore EG, Gibson QH. J Biol Chem 1976;251:2788–2794. [PubMed: 1262343]
67. Traylor TG, Sharma VS. Biochemistry 1992;31:2847–2849. [PubMed: 1348002]
68. Brucker EA, Olson JS, Ikeda-Saito M, Phillips GN Jr. Proteins: Struct, Funct, Genet 1998;30:352–356. [PubMed: 9533619]
69. Zhao Y, Brandish PE, Ballou DP, Marletta MA. Proc Natl Acad Sci U S A 1999;96:14753–14758. [PubMed: 10611285]
70. Sharma VS, Magde D. Methods 1999;19:494–505. [PubMed: 10581149]
71. MacNeil JH, Berseth PA, Bruner EL, Perkins TL, Wadia Y, Westwood G, Trogler WC. J Am Chem Soc 1997;119:1668–1675.
72. Pinakoulaki E, Stavrakis S, Urbani A, Varotsis C. J Am Chem Soc 2002;124:9378–9379. [PubMed: 12167025]
73. Blomberg ML, Blomberg MRA, Siegbahn PEM. Biochem Biophys Acta 2006;1757:31–46. [PubMed: 16375849]
74. Blomberg LM, Blomberg MR, Siegbahn PE. Biochim Biophys Acta 2006;1757:240–252. [PubMed: 16774734]
75. Moënne-Loccoz P, Richter O-MH, Huang HW, Wasser IM, Ghiladi RA, Karlin KD, de Vries S. J Am Chem Soc 2000;122:9344–9345.
76. Sanders-Loehr J, Wheeler WD, Shiemke AK, Averill BA, Loehr TM. J Am Chem Soc 1989;111:8084–8093.
77. Martens CF, Murthy NN, Obias HV, Karlin KD. Chem Commun 1996:629–630.
78. Field SJ, Prior L, Roldán MD, Cheesman MR, Thomson AJ, Spiro S, Butt JN, Watmough NJ, Richardson DJ. J Biol Chem 2002;277:20146–20150. [PubMed: 11901154]
79. Iwata S, Ostermeier C, Ludwig B, Michel H. Nature 1995;376:660–669. [PubMed: 7651515]
80. Tsukihara T, Aoyama H, Yamashita E, Tomizaki T, Yamaguchi H, Shinzawa-Itoh K, Nakashima R, Yaono R, Yoshikawa S. Science 1995;269:1069–1074. [PubMed: 7652554]
81. Tsukihara T, Aoyama H, Yamashita E, Tomizaki T, Yamaguchi H, Shinzawa I-K, Nakashima R, Yaono R, Yoshikawa S. Science 1996;272:1136–1144. [PubMed: 8638158]
82. Ostermeier C, Harrenga A, Ermler U, Michel H. Proc Natl Acad Sci U S A 1997;94:10547–10553. [PubMed: 9380672]
83. Soulimane T, Buse G, Bourenkov GP, Bartunik HD, Huber R, Than ME. EMBO J 2000;19:1766–1776. [PubMed: 10775261]
84. Feig AL, Lippard SJ. Chem Rev 1994;94:759–805.
85. Solomon EI, Tuczek F, Root DE, Brown CA. Chem Rev 1994;94:827–856.
86. Wallar BJ, Lipscomb JD. Chem Rev 1996;96:2625–2658. [PubMed: 11848839]
87. Silaghi-Dumitrescu R, Kurtz DM Jr, Ljungdahl LG, Lanzilotta WN. Biochemistry 2005;44:6492–6501. [PubMed: 15850383]
88. Haskin CJ, Ravi N, Lynch JB, Münck E, Que L Jr. Biochemistry 1995;34:11090–11098. [PubMed: 7669766]
89. Coufal DE, Tavares P, Pereira AS, Hyunh BH, Lippard SJ. Biochemistry 1999;38:4504–4513. [PubMed: 10194372]

90. Silaghi-Dumitrescu R, Coulter ED, Das A, Ljungdahl LG, Jameson GN, Huynh BH, Kurtz DM Jr. Biochemistry 2003;42:2806–2815. [PubMed: 12627946]
91. Wyllie GR, Schulz CE, Scheidt WR. Inorg Chem 2003;42:5722–5734. [PubMed: 12950223]
92. Chan NL, Kavanaugh JS, Rogers PH, Arnone A. Biochemistry 2004;43:118–132. [PubMed: 14705937]
93. Nakamoto, K. Infrared and Raman spectroscopy of inorganic and coordination compounds. 5. John Wiley and Sons Inc.; New York: 1997.
94. Schlichting I, Berendzen J, Phillips GN Jr, Sweet RM. Nature 1994;371:808–812. [PubMed: 7935843]
95. Teng TY, Srajer V, Moffat K. Nat Struct Biol 1994;1:701–705. [PubMed: 7634074]
96. Hartmann H, Zinser S, Komninos P, Schneider RT, Nienhaus GU, Parak F. Proc Natl Acad Sci U S A 1996;93:7013–7016. [PubMed: 8692935]
97. Alben JO, Beece D, Bowne SF, Doster W, Eisenstein L, Frauenfelder H, Good D, McDonald JD, Marden MC, Moh PP, Reinisch L, Reynolds AH, Shyamsunder E, Yue KT. Proc Natl Acad Sci U S A 1982;79:3744–3748. [PubMed: 6954517]
98. Fiamingo FG, Alben JO. Biochemistry 1985;24:7964–7970. [PubMed: 4092047]
99. Ansari A, Berendzen J, Braunstein D, Cowen BR, Frauenfelder H, Hong MK, Iben IE, Johnson JB, Ormos P, Sauke TB, Scholl R, Schulte A, Steinbach PJ, Vittitow J, Young RD. Biophys Chem 1987;26:337–355. [PubMed: 3607234]
100. Alben JO, Moh PP, Fiamingo FG, Altschuld RA. Proc Natl Acad Sci U S A 1981;78:234–237. [PubMed: 6264435]
101. Woodruff WH, Dallinger RF, Antalis TM, Palmer G. Biochemistry 1981;20:1332–1338. [PubMed: 6261789]
102. Einarsdóttir Ó, Killough PM, Fee JA, Woodruff WH. J Biol Chem 1989;264:2405–2408. [PubMed: 2536707]
103. Dyer RB, Einarsdóttir Ó, Killough PK, López-Garriga JJ, Woodruff WH. J Am Chem Soc 1989;111:7657–7659.
104. Hendriks J, Warne A, Gohlke U, Haltia T, Ludovici C, Lübben M, Saraste M. Biochemistry 1998;37:13102–13109. [PubMed: 9748316]
105. Lu, S. Ph. D. thesis, Department of Environmental & Biomolecular Systems, OGI School of Science&Engineering, Oregon Health&Science University. 2005. Characterization of nitrosyl, azido, and carbonyl complexes in diiron enzymes and their implications for O_2 and NO activation.
106. Hendriks JH, Prior L, Baker AR, Thomson AJ, Saraste M, Watmough NJ. Biochemistry 2001;40:13361–13369. [PubMed: 11683646]
107. Koutsoupakis K, Stavrakis S, Soulimane T, Varotsis C. J Biol Chem 2003;278:14893–14896. [PubMed: 12594218]
108. Pinakoulaki E, Varotsis C. Biochemistry 2003;42:14856–14861. [PubMed: 14674760]
109. Wasser IM, Huang HW, Moënne-Loccoz P, Karlin KD. J Am Chem Soc 2005;127:3310–3320. [PubMed: 15755147]
110. Suharti. Ph. D. thesis, Department of Biotechnology, Delft University of Technology. 2005. qCu_ANOR a novel bifunctional nitric oxide reductase from Bacillus azotoformans.
111. Rosenzweig AC, Frederick CA, Lippard SJ, Nordlund P. Nature 1993;366:537–543. [PubMed: 8255292]
112. Rosenzweig AC, Nordlund P, Takahara PM, Frederick CA, Lippard SJ. Chem Biol 1995;2:409–418.
113. Whittington DA, Sazinsky MH, Lippard SJ. J Am Chem Soc 2001;123:1794–1795. [PubMed: 11456795]
114. Nordlund P, Sjöberg B-M, Eklund H. Nature 1990;345:593–598. [PubMed: 2190093]
115. Nordlund P, Eklund H. J Mol Biol 1993;232:123–164. [PubMed: 8331655]
116. Logan DT, Su XD, Aberg A, Regnstrom K, Hajdu J, Eklund H, Nordlund P. Structure 1996;4:1053–1064. [PubMed: 8805591]

117. Pulver S, Froland WA, Fox BG, Lipscomb JD, Solomon EI. J Am Chem Soc 1993;115:12409–12422.
118. Pulver SC, Froland WA, Lipscomb JD, Solomon EI. J Am Chem Soc 1997;119:387–395.
119. Fox BG, Lyle KS, Rogge CE. Acc Chem Res 2004;37:421–429. [PubMed: 15260504]
120. Rardin RL, Tolman WB, Lippard SJ. New J Chem 1991;15:417–430.
121. Sakurai T, Sakurai N, Matsumoto H, Hirota S, Yamauchi O. Biochem Biophys Res Commun 1998;251:248–251. [PubMed: 9790940]
122. Lu S, Libby E, Saleh L, Xing G, Bollinger JM Jr, Moënne-Loccoz P. J Biol Inorg Chem 2004;9:818–827. [PubMed: 15311337]
123. Koutsoupakis K, Stavrakis S, Pinakoulaki E, Soulimane T, Varotsis C. J Biol Chem 2002;277:32860–32866. [PubMed: 12097331]
124. Pinakoulaki E, Gemeinhardt S, Saraste M, Varotsis C. J Biol Chem 2002;277:23407–23413. [PubMed: 11971903]
125. Sakurai T, Nakashima S, Kataoka K, Seo D, Sakurai N. Biochem Biophys Res Commun 2005;333:483–487. [PubMed: 15950940]
126. Wang YN, Averill BA. J Am Chem Soc 1996;118:3972–3973.
127. Miller LM, Pedraza AJ, Chance MR. Biochemistry 1997;36:12199–12207. [PubMed: 9315857]
128. Mukai M, Ouellet Y, Ouellet H, Guertin M, Yeh SR. Biochemistry 2004;43:2764–2770. [PubMed: 15005611]
129. Torres J, Cooper CE, Wilson MT. J Biol Chem 1998;273:8756–8766. [PubMed: 9535853]
130. Cooper CE. Trends Biochem Sci 2002;27:33–39. [PubMed: 11796222]
131. Brunori M, Giuffrè A, Forte E, Mastronicola D, Barone MC, Sarti P. Biochim Biophys Acta 2004;1655:365–371. [PubMed: 15100052]
132. Brunori M, Forte E, Arese M, Mastronicola D, Giuffrè A, Sarti P. Biochim Biophys Acta 2006;1757:1144–1154. [PubMed: 16792997]
133. Stevens TH, Brudvig GW, Bocian DF, Chan SI. Proc Natl Acad Sci U S A 1979;76:3320–3324. [PubMed: 226967]
134. Brudvig GW, Stevens TH, Chan SI. Biochemistry 1980;19:5275–5285. [PubMed: 6255988]
135. Torres J, Cooper CE, Sharpe M, Wilson MT. J Bioenerg Biomembr 1998;30:63–69. [PubMed: 9623807]
136. Torres J, Sharpe MA, Rosquist A, Cooper CE, Wilson MT. FEBS Lett 2000;475:263–266. [PubMed: 10869568]
137. Butler C, Forte E, Maria Scandurra F, Arese M, Giuffrè A, Greenwood C, Sarti P. Biochem Biophys Res Commun 2002;296:1272–1278. [PubMed: 12207912]
138. Brunori M, Giuffrè A, Sarti P, Stubauer G, Wilson MT. Cell Mol Life Sci 1999;56:549–557. [PubMed: 11212305]
139. Zhao XJ, Sampath V, Caughey WS. Biochem Biophys Res Commun 1994;204:537–543. [PubMed: 7980511]
140. Forte E, Urbani A, Saraste M, Sarti P, Brunori M, Giuffrè A. Eur J Biochem 2001;268:6486–6491. [PubMed: 11737203]
141. Brown GC. Biochim Biophys Acta 2001;1504:46–57. [PubMed: 11239484]
142. Pearce LL, Bominaar EL, Hill BC, Peterson J. J Biol Chem 2003;278:52139–52145. [PubMed: 14534303]
143. Pinakoulaki E, Ohta T, Soulimane T, Kitagawa T, Varotsis C. J Am Chem Soc 2005;127:15161–15167. [PubMed: 16248657]
144. Ohta T, Kitagawa T, Varotsis C. Inorg Chem 2006;45:3187–3190. [PubMed: 16602774]
145. Bau R, Sabherwal IH, Burg AB. J Am Chem Soc 1971;93:4926–4928.
146. Arulsamy N, Bohle DS, Imonigie JA, Levine S. Angew Chem, Int Ed 2002;41:2371–2373.
147. Bottcher HC, Graf M, Mereiter K, Kirchner K. Organometallics 2004;23:1269–1273.
148. Bottcher HC, Wagner C, Kirchner K. Inorg Chem 2004;43:6294–6299. [PubMed: 15446875]
149. Moody AJ. Biochim Biophys Acta 1996;1276:6–20. [PubMed: 8764888]

150. Scott RA, Li PM, Chan SI. Ann N Y Acad Sci 1988;550:53–58. [PubMed: 2854411]
151. Li PM, Gelles J, Chan SI, Sullivan RJ, Scott RA. Biochemistry 1987;26:2091–2095. [PubMed: 3040080]
152. Ralle M, Verkhovskaya ML, Morgan JE, Verkhovsky MI, Wikström M, Blackburn NJ. Biochemistry 1999;38:7185–7194. [PubMed: 10353829]
153. Fabian M, Skultety L, Brunel C, Palmer G. Biochemistry 2001;40:6061–6069. [PubMed: 11352742]
154. Li W, Palmer G. Biochemistry 1993;32:1833–1843. [PubMed: 8382524]
155. Orii Y, Mogi T, Sato-Watanabe M, Hirano T, Anraku Y. Biochemistry 1995;34:1127–1132. [PubMed: 7827061]
156. Gardner AM, Helmick RA, Gardner PR. J Biol Chem 2002;277:8172–8177. [PubMed: 11751865]
157. Gomes CM, Giuffrè A, Forte E, Vicente JB, Saraiva LM, Brunori M, Teixeira M. J Biol Chem 2002;277:25273–25276. [PubMed: 12101220]
158. Iyer RB, Silaghi-Dumitrescu R, Kurtz DM Jr, Lanzilotta WN. J Biol Inorg Chem 2005;10:407–416. [PubMed: 15895271]

Biography

Pierre Moënne-Loccoz was born in France in 1964. He received his PhD in 1989 from Université Pierre et Marie Curie (Paris, France) for his work on Photosystem I and II of higher plants, under the supervision of Marc Lutz and Bruno Robert (CE Saclay, France). He continued to study photoactive proteins, first with Warner Peticolas at the University of Oregon and then with Mike Evans and Peter Heathcote at University College London. He then joined Thomas Loehr and Joann Sanders-Loehr at the Oregon Graduate Institute, where he started investigating O_2-activation processes in heme and non-heme diiron proteins. He is now an Assistant Professor at the OGI School of Engineering at OHSU where he continues to work on O_2 and NO chemistry in metalloproteins using a variety of spectroscopic techniques.

Pierre Moënne-Loccoz

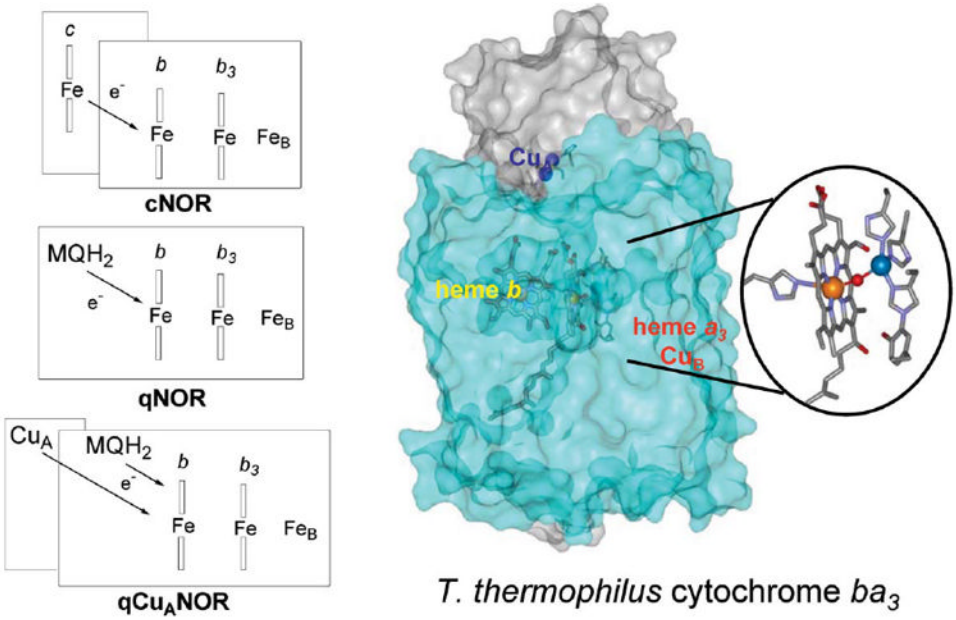

Fig. 1.

Schematic representations of 3 subfamilies of NO reductases, and the X-ray structure of *T. thermophilus* cytochrome ba_3 (based on coordinates from ref. [83]).

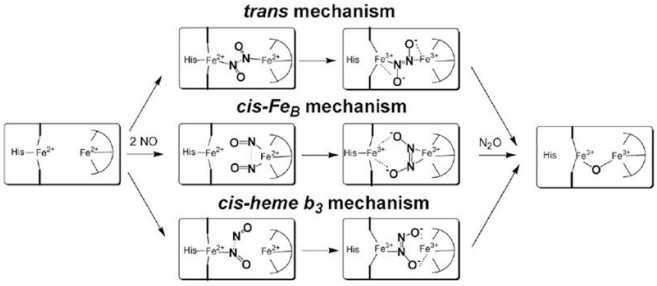

Fig. 2.
Putative mechanisms of NO reductase.

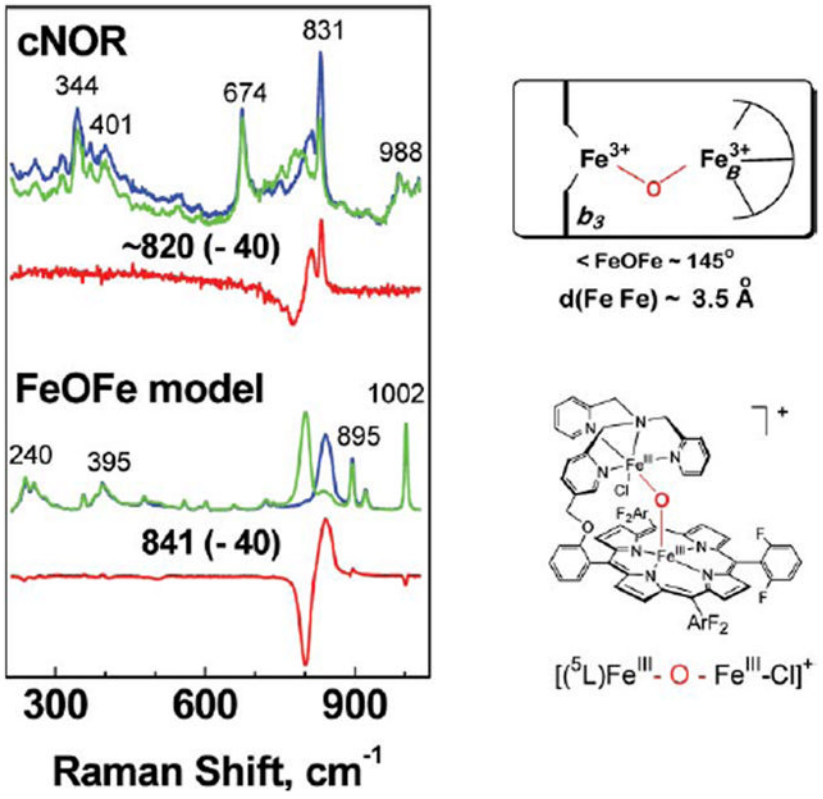

Fig. 3.

Resonance Raman characterization of heme/non-heme μ-oxo bridged diiron(III) cluster in oxidized cNOR (in $^{16}OH_2$ (blue), $^{18}OH_2$ (green) and difference spectrum (red)), and in a synthetic model in CH_3CN with 20% water (in $^{16}OH_2$ (blue), $^{18}OH_2$ (green) and difference spectrum (red)). The ν_{as}(Fe–O–Fe) modes are identified by their 40 cm^{-1} downshift upon exchange of the O-atom with ^{18}O-labeled water. The schematic structures of the diiron clusters in cNOR and the model compound are also shown (adapted from ref. [75]).

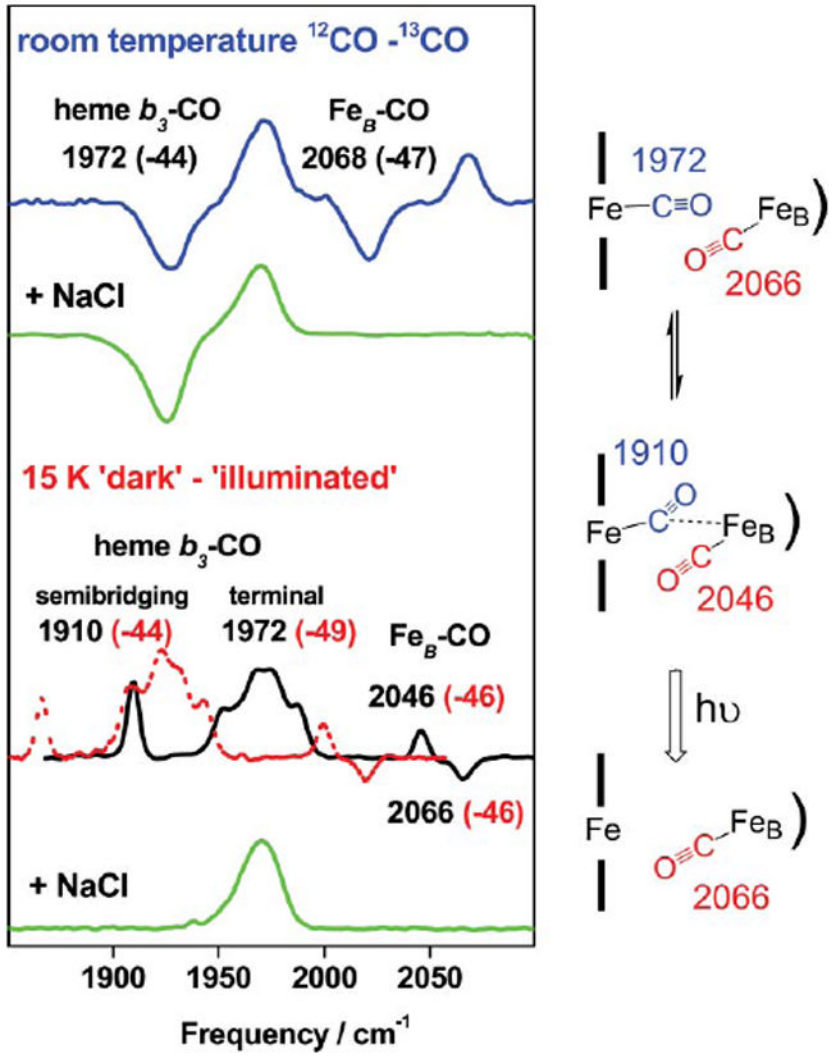

Fig. 4.

FTIR difference spectra of qCu$_A$NOR–CO. At room temperature (top traces), the *v*(CO) are isolated using ^{12}CO–^{13}CO spectra (blue trace: no chloride added, green trace: 3 M chloride). At 15 K (bottom traces), 'dark' minus 'illuminated' spectra reveal photosensitive *v*(CO) modes (black trace: ^{12}CO; red trace: ^{13}CO; and green trace: ^{12}CO in the presence of 3 M NaCl). A schematic interpretation of the binding of CO in qCu$_A$ NOR is also shown (adapted from ref. [57]).